is achieved when the proportion of the four-coordinate copper sites **3a** in the Cu1 atom plane exceeds a certain minimum value. An important implication of these observations is that the superconductivity at $T_c \simeq 93$ K might originate from the formation of Cooper pairs (i.e., pairs of electrons that are charge carriers of superconductors) between electrons of the Cu2 atoms across the Cu2-O4-Cu1-O4-Cu2 linkages as illustrated in **4**.[30] When

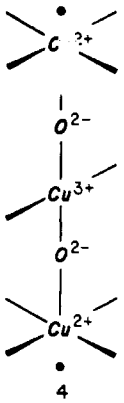

4

such a Cooper pair formation is unfavorable by lengthening the Cu2-O4-Cu1-O4-Cu2 linkages, Cooper pairs may be formed between the electrons of the Cu2 atoms within each CuO_2 layer, a situation identical with that in the CuO_4 layers of doped superconductors $La_{2-x}M_xCuO_4$. Future theories aimed at describing the high-temperature superconductivity in $YBa_2Cu_3O_{7-y}$ must take into consideration the interlayer interaction mediated by the Cu2-O4-Cu1-O4-Cu2 linkages.

One possible reason for why tetragonal $YBa_2Cu_3O_{7-y}$ ($y > 0.5$) is not superconducting might be that its CuO_2 layer $x^2 - y^2$ band remains half-filled, which requires that the Cu1 atom plane contain the Cu^{3+} and Cu^+ cations in the $(1 - y):y$ ratio. If this is the case, tetragonal $YBa_2Cu_3O_{7-y}$ ($y > 0.5$) would be semiconducting, as shown by van den Berg et al.,[16] and exhibit an antiferromagnetic ordering. We also note that tetragonal $YBa_2Cu_3O_6$ is found to be semiconducting.[6d,7b]

Our calculations of the crystal energies for orthorhombic and tetragonal $YBa_2Cu_3O_{7-y}$ suggest that formation of CuO_3 chains in orthorhombic $YBa_2Cu_3O_{7-y}$ ($y < 0.5$) may arise from two energy factors: to avoid a right-angle arrangement of two oxygen atoms around each Cu1 atom within the Cu1 atom plane and to avoid a T-shape three-coordination for copper. Even for tetragonal $YBa_2Cu_3O_{7-y}$ ($y > 0.5$), these energy factors may still be operative. Thus it is possible that the presence of enough oxygen atom vacancies in tetragonal $YBa_2Cu_3O_{7-y}$ ($y > 0.5$) may allow some short CuO_3 chains to exist and hence some Cu^{3+} sites to form randomly in the two orthogonal directions of the Cu1 atom plane, which leads to a tetragonal structure on a statistical basis.

Acknowledgment. Work at North Carolina State University and Argonne National Laboratory was supported by the Office of Basic Energy Sciences, Division of Materials Sciences, U.S. Department of Energy, under Grant DE-FG05-86-ER45259 and under Contract W-31-109-ENG-38, respectively. We express our appreciation for computing time made available by DOE on the ER-Cray X-MP computer, and would also like to thank Dr. J. D. Jorgensen for preprints of his work, Dr. W. R. Busing for making his WMIN program available to us and also for his invaluable advice concerning how to use it, and Dr. D. Wolf for references.

Contribution from the Department of Chemistry, University of California, Berkeley, California 94720

Ferric Ion Sequestering Agents. 18.[1] Two Dihydroxamic Acid Derivatives of EDTA and DTPA

Petra N. Turowski, Steven J. Rodgers,† Robert C. Scarrow, and Kenneth N. Raymond*

Received November 14, 1986

Two new dihydroxamate analogues of the siderophore aerobactin, derived from the polyamine carboxylate ligands EDTA (ethylenediaminetetraacetic acid) and DTPA (diethylenetriaminepentaacetic acid), have been synthesized. The protonation and stability constants of the ligands and of their complexes with iron(III) have been determined by using potentiometric methods. The number of species in solution and the metal-ligand protonation constants were independently determined by a linear algebraic analysis and least-squares refinement of the visible absorption spectra. The metal-ligand formation constants, K_{ML}, were determined from a similar analysis of the ultraviolet spectra near pH 1. These formation constants [log K values of 30.2 (6) and 29.7 (7), respectively] are higher than usual for dihydroxamate ligands, and there is some evidence that the new ligands may be effective iron removal agents in vivo. The ligands are easily made and purified in large quantities and have desirable solubility properties.

Introduction

We have been involved in the synthesis of ligands that might be useful in the metal chelation therapy of iron overload[2] and, in a related project, the preparation of specific sequestering agents for plutonium.[3] For this purpose, we have looked to the siderophores—a class of molecules produced by microorganisms to acquire sufficient iron for their survival—for examples of highly specific sequestering agents.[4] Two major groups of siderophores are the catecholates, such as enterobactin, and the hydroxamates, exemplified by the ferrioxamines, aerobactin, and others. Our attention has focused mainly on ligands mimicking enterobactin, since it is the strongest iron(III) chelating agent known (log K_{ML} = 52).[5] Unfortunately, such tricatecholate ligands are often difficult and expensive to synthesize and the parent compounds and their ferric complexes are relatively insoluble in neutral and acidic solutions.[6] This is also true for the larger trihydroxamate ligands, since the backbone of such ligands often consists of fairly large nonpolar or only slightly polar chains and rings that enable the chelating moieties to bind all the coordination sites of the metal.

* To whom correspondence should be addressed.
† Deceased.

(1) Part 17: McMurry, T. J.; Hasseini, M. W.; Garrett, T. M.; Hahn, F. E.; Reyes, Z. E.; Raymond, K. N. *J. Am. Chem. Soc.* **1987**, *101*, 7196.
(2) Raymond, K. N.; Chung, T. D. Y.; Pecoraro, V. L.; Carrano, C. J. *The Biochemistry and Physiology of Iron*; Saltman, P., Hegenauer, J., Eds.; Elsevier Biomedical: New York, 1982; pp 649-662.
(3) A discussion of the chemical and biochemical similarities of iron and plutonium may be found in: Raymond, K. N.; Smith, W. L. *Structure and Bonding*; Goodenough, J. B., Hemmerich, P., Ibers, J. A., Jorgenson, C. K., Neilands, J. B., Reinen, D., Williams, R. J. P., Eds.; Springer-Verlag: West Berlin, 1981; Vol. 43, pp 159-186.
(4) A recent review of this may be found in: Raymond, K. N.; Müller, G.; Matzanke, B. F. *Topics in Current Chemistry*; Boschke, F. L., Ed.; Springer-Verlag: West Berlin, 1984; Vol. 123, pp 49-102.
(5) Harris, W. R.; Carrano, C. J.; Cooper, S. R.; Sofen, S. R.; Afdeef, A. E.; McArdle, J. V.; Raymond, K. N. *J. Am. Chem. Soc.* **1979**, *101*, 6097.
(6) Harris, W. R.; Raymond, K. N. *J. Am. Chem. Soc.* **1979**, *101*, 6534.

0020-1669/88/1327-0474$01.50/0

In contrast, amine carboxylate ligands such as EDTA and DTPA are zwitterionic and have very good solubility properties. Both EDTA and DTPA have been used in chelation therapy for some time.[7] In addition to its use in complexing other toxic metals such as Pb(II), EDTA has been used with moderate success in the treatments of primary hemochromatosis and iron-loading anemias.[7] The salts of DTPA have been used to complex metal ions with higher coordination numbers, especially the transuranium elements. A major disadvantage of the polycarboxylates is that they also bind to other essential metal ions, notably zinc and calcium, causing their depletion in vivo. These effects have been partly offset by administering the ligands as metal salts; Ca-DTPA is the current drug used for plutonium decontamination.[8] By incorporation of more metal ion specificity into the coordinating groups of EDTA and DTPA, economic, soluble ligands with applications in iron and plutonium chelation therapy may be synthesized.

Here we report the preparation of bis(*N*-isopropylhydroxamate) derivatives of EDTA and DTPA. These molecules resemble the dihydroxamate siderophore aerobactin (**1**). They form 1:1 complexes with iron(III) that are as stable as, or more stable than, those of dihydroxamate siderophores. These complexes protonate in neutral and acidic solution to form MHL and MH_2L species and deprotonate to MOHL at high pH. The ligands and complexes are quite soluble in aqueous media from pH 1 to 11. The synthesis of the unsubstituted dihydroxamate derivative of EDTA (EDTA-DX, **2**) has been reported.[9,10]

Experimental Section

Materials. Analytical reagents were used as supplied. Reagent grade tetrahydrofuran (THF) was distilled over sodium–benzophenone ketyl. The dimethyl sulfoxide (DMSO) used was spectral grade; other solvents were reagent grade and were used as supplied. The dianhydrides of EDTA and DTPA were prepared from EDTA or DTPA and acetic anhydride in pyridine by using published methods.[11] *N*-isopropylhydroxylamine was prepared by a procedure similar to the one used to make dihydroxamate derivatives of aliphatic dicarboxylic acids.[12] Specifically, 460 g (7.1 mol) of Zn dust was added over a period of 30 min to a stirred solution of 270 mL of 2-nitropropane (2.9 mol) and 120 g of NH_4Cl in 1500 mL of H_2O, which was cooled in an ice bath. After it was stirred for a total period of 4 h, the mixture was filtered and the aqueous filtrate was extracted with 7 × 500 mL of CH_2Cl_2. The organic fractions were combined and dried over Na_2SO_4 and the solvent was removed in vacuo below 0 °C to yield, after washing with hexane, 83 g (30–40%) of slightly wet colorless needles.

For titration studies, ferric nitrate and ferric perchlorate solutions were prepared and standardized as described earlier.[13] The iron content of the ferric solutions was determined by potentiometric titrations with $Na_2H_2EDTA{\cdot}2H_2O$ (recrystallized from hot water). Acid and base solutions (0.1 M HNO_3 and KOH) were made by using Baker Dilut-it ampules and standardized.[13] The ionic strength of the titration solutions was adjusted to 0.10 M by the addition, as necessary, of KNO_3 (recrystallized from hot water). (The solution temperature was maintained at 25.0 ± 0.5 °C by a circulating water bath.)

Preparation of Ethylenedinitrilo-*N*,*N*′-diacetic-*N*,*N*′-bis(*N*-2-propylacetohydroxamic) Acid, *i*-Pr_2EDTA-DX (3). In a manner similar to the synthesis of earlier ligands,[9] *N*-isopropylhydroxylamine (29 g, 390 mmol) was added to the dianhydride of EDTA (10 g, 39 mmol) dissolved in 250 mL of DMSO using Schlenk techniques and maintained under a nitrogen atmosphere at room temperature for 4 days. Most of the solvent was removed on a rotary evaporator in vacuo at 70 °C to yield a beige amorphous mass. To this was added THF (250 mL), and the mixture was stirred vigorously until the remaining DMSO and hydroxylamine went into solution and only a finely divided white precipitate remained. This precipitate (15 g, 96%) was filtered and recrystallized from methanol/ethyl ether to yield a fluffy white solid, **3** (9.7 g, 61%), which decomposes to a brown solid above 195 °C. Anal. Calcd for $C_{16}H_{10}N_4O_8$: C, 47.28; H, 7.44; N, 13.79. Found: C, 46.99; H, 7.42; N, 13.72. ^{1}H NMR (DMSO-d_6): δ 1.06 (d, J = 6 Hz, 12 H), 2.87 (br m, 4 H), 3.47 (s, 4 H), 3.72 (s, 4 H), 4.50 (septuplet, J = 6 Hz, 2 H). FAB-MS (m/e): 407 (M + H), 391, 349, 217, 203. IR (cm^{-1}): 1688, 1650, 1606.

Preparation of Diethylenetrinitrilo-*N*,*N*′,*N*″-triacetic-*N*,*N*″-bis(*N*-2-propylacetohydroxamic) Acid, *i*-Pr_2DTPA-DX (4). *N*-Isopropylhydroylamine (21 g, 270 mmol) and the dianhydride of DTPA (10 g, 28 mmol) were combined and the product worked up as above. After recrystallization from methanol/ethyl ether a white fluffy hygroscopic solid (10 g, 73%) was obtained, which loses H_2O after heating in vacuo at 70 °C for 3 days and decomposes to a brown solid above 131 °C. Anal. Calcd for $C_{20}H_{37}N_5O_{10}{\cdot}H_2O$: C, 45.70; H, 7.48; N, 13.33. Found: C, 45.93; H, 7.21; N, 13.15. ^{1}H NMR (DMSO-d_6): δ 1.06 (d, J = 6 Hz, 12 H), 3.02 (br m, 4 H), 3.17 (br m, 4 H), 3.50 (s, 4 H), 3.67 (s, 2 H), 3.75 (s, 4 H), 4.51 (septuplet, J = 6 Hz, 2 H). FAB-MS (m/e): 508 (M + H), 450, 217, 203, 201. IR (cm^{-1}): 1720, 1640.

Preparation of Ethylenedinitrilo-*N*,*N*′,*N*′-triacetic-(*N*-2-propylacetohydroxamic) Acid *N*′-2-Propylamino Ester (5). The dianhydride of EDTA (0.60 g, 2.3 mmol) was added to *N*-isopropylhydroxylamine (0.53 g, 7.0 mmol) dissolved in THF (75 mL) and the heterogeneous mixture stirred under N_2 at room temperature for 2 days. The resulting finely divided white solid (0.85 g, 90%) was filtered and dried in vacuo. Anal. Calcd: see analysis for **3**. Found: C, 47.42; H, 7.35; N, 13.58. ^{1}H NMR (DMSO-d_6): δ 0.95 (d, J = 6 Hz, 6 H), 1.07 (d, J = 6 Hz, 6 H), 2.85 (br m, 4 H), 3.17 (septuplet, J = 6 Hz, 1 H), 3.45 (s, 2 H), 3.49 (s, 2 H), 3.61 (s, 2 H), 3.75 (s, 2 H), 4.51 (septuplet, J = 6 Hz, 1 H). IR (cm^{-1}): 1730, 1640.

Instruments. Nuclear magnetic resonance spectra in DMSO-d_6 were obtained on 200- and 250-MHz Fourier transform instruments employing modified Nicolet software and using Me_4Si as a reference standard. Infrared spectra were obtained on a Perkin-Elmer Model 597 spectrophotometer calibrated with polystyrene film. Positive fast-atom-bombardment (argon) mass spectra from a thioglycerol matrix were detected by an AEI MS-12 instrument. Mass spectra and microanalyses were performed by the Analytical Services Laboratory, Chemistry Department, University of California, Berkeley, CA. For pH measurements, a Fisher Accumet pH meter, Model 825MP, equipped with a Sigma E-4753 ("Trizma") combination electrode, was used. Before each titration, the electrode was calibrated with standardized 0.004 M or 0.1 M HNO_3 and 0.004 M KOH solutions adjusted to 0.100 M ionic strength to read the concentration, not the activity, of hydrogen ion.

Potentiometric Titrations. Titrations were performed as described previously.[13] The titrant used was 0.1 M KOH, and the ferric nitrate and HNO_3 solutions were added by using calibrated 2.0 -mL Gilmont burets. The solution temperature was maintained at 25 ± 0.5 °C by a circulating water bath. Before titration, solutions were degassed with argon that had been bubbled through a basic solution of pyrogallol. Typically, a 0.4 mM solution of ligand with an equivalent of acid at pH 3.3 was titrated with 0.1 M KOH to pH 10.5. For titrations of the ferric complexes, ferric stock solutions were added to the ligands to give approximately 0.98 equiv of Fe^{3+} and 1.2 equiv of excess acid. This solution (pH 2.9) was again titrated with 0.1 M KOH to pH 11.

Nuclear Magnetic Resonance pH Titrations. NMR pH titrations in D_2O were carried out on a Varian XL 300 Fourier transform instrument at an ambient temperature of 23 ± 1 °C, using $NaO_3(CH_2)_3Si(Me)_3$ (TSP, δ = 0.015) as an internal reference standard. Stock solutions of the free ligands (7–20 mM) were prepared by dissolving appropriate amounts of the ligands in 0.1 M DCl in D_2O. The pH of the stock solutions were adjusted by the addition of 30% NaOD in D_2O and 20% DCl in D_2O, as necessary. From pH 0.5 to 3.5, spectra were obtained at intervals of 0.1 pH unit and from pH 0 to 12 at intervals of approximately 1 pH unit.

Spectrophotometric Titrations. All spectra were measured on a Hewlett-Packard 8450A UV–vis multichannel digital spectrophotometer equipped with a Model 8901A temperature controller. The solution temperature was maintained at 25 ± 0.5 °C by a circulating water bath. Additions of stock solutions and of titrant were made by using 2.0-mL calibrated Gilmont burets. To determine protonation constants of the metal–ligand complexes, a 1:1.1 mixture (0.1–0.4 mM) of iron(III) and ligand was titrated with 0.1 M HNO_3 from pH 10.4 to 3.3 and with 10 M NaOH from pH 1 to 11.3 (the initial electrolyte was 0.10 M HCl). To determine the metal–ligand stability constants, ligand additions were made to a solution of ferric perchlorate (0.16 mM) at pH 1 (HCl).

Results

Syntheses. The bis(isopropylhydroxamic acid) derivatives of EDTA and DTPA were made in two steps (see the bottom of

(7) For applications with iron, see: Martell, A. E., Anderson, D. C., Badman, D. C., Eds. *Development of Iron Chelators for Clinical Use*; Elsevier/North-Holland: Amsterdam, 1981.
(8) Lushbaugh, C. C.; Washburn, L. C. *Health Phys.* **1979**, *36*, 472.
(9) Motekaitis, R. J.; Murase, I.; Martell, A. E. *J. Coord. Chem.* **1971**, *1*, 77.
(10) Herz, J. L.; Chaberek, S. U.S. Patent 3 859 337, 1975.
(11) Geigy, J. R. A.-G. Fr. Patent 1 548 888 (Cl. C 07d), 1968; *Chem. Abstr.* **1969**, *71*, 81380q.
(12) Smith, W. L.; Raymond, K. N. *J. Am. Chem. Soc.* **1980**, *102*, 1252.
(13) Scarrow, R. C.; Riley, P. E.; Abu-Dari, K.; White, D. L.; Raymond, K. N. *Inorg. Chem.* **1985**, *24*, 954.

Table I. Stability Constants[a]

Ligand Protonation Constants

constant	*i*-Pr_2EDTA-DX (3)	*i*-Pr_2DTPA-DX (4)	constant	*i*-Pr_2EDTA-DX (3)	*i*-Pr_2DTPA-DX (4)
log K_1	10.56 (1)	10.85 (3)	log K_5	1.7 (5)	3.70 (3)
log K_2	9.67 (1)	10.10 (3)	log K_6	0.7 (5)	2.07 (5)
log K_3	8.03 (1)	9.07 (3)	log K_7		1.3 (5)
log K_4	4.20 (10)	5.94 (3)	log K_8		0.0 (5)

Complex Protonation Constants

	i-Pr_2EDTA-DX (3)			*i*-Pr_2DTPA-DX (4)		
constant	potentiometric	spectral	reported	potentiometric	spectral	reported
log K^{H}_{MOHL}[c]	−10.27 (1)	−10.33 (2)	−10.30 (3)	−9.93 (1)	−9.92 (7)	−9.93 (1)
log K^{H}_{MHL}[d]	4.26 (1)	4.23 (2)	4.24 (2)	8.10 (1)	8.15 (2)	8.12 (3)
log $K^{H}_{MH_2L}$[e]	4.71 (1)	4.58 (8)	4.65 (6)	6.15 (1)	6.10 (1)	6.12 (2)

Complex Formation Constants[f]

	i-Pr_2EDTA-DX (3)	*i*-Pr_2DTPA-DX (4)
log β_{MH_2L}[b]	39.1 (-)	4 (-)
log K_{ML}[g]	30.2 (-)	29.7 (-)

[a] Standard deviations are given in parentheses and correspond to the error in the last digit(s). No correlation coefficients between any two log K values exceed 0.34. [b] Defined in the text. [c] K^{H}_{MOHL} = [MOHL][H]/[ML]. [d] K^{H}_{MHL} = [MHL]/[ML][H]. [e] $K^{H}_{MH_2L}$ = [MH_2L]/[MHL][H]. [f] Standard deviations of the values are due to the uncertainties of the carboxylate log K values. Errors due to the refinement data are ±0.4 log unit for *i*-Pr_2EDTA-DX and ±0.03 log unit for *i*-Pr_2DPTA-DX. [g] K_{ML} = [ML]/[M][L].

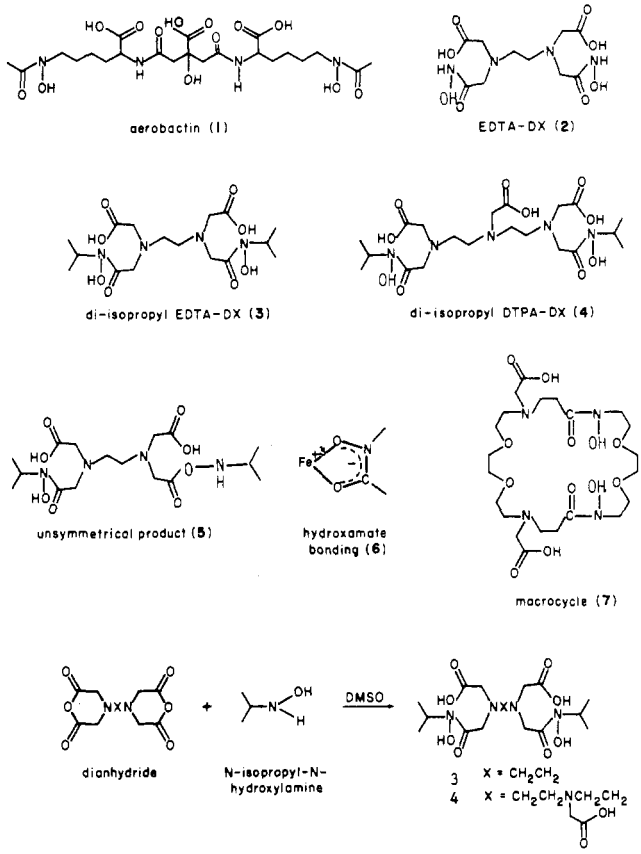

Figure 1. Structures and contracted names of the compounds described and a reaction scheme of the ligand synthesis.

Figure 1). The dianhydrides of the amine carboxylic acids were prepared by using literature methods[11] and subsequently were conjugated with 2 equiv of *N*-isopropylhydroxylamine in DMSO to make the dihydroxamate ligands *i*-Pr_2EDTA-DX (**3**) and *i*-Pr_2DTPA-DX (**4**) (Figure 1). These are easily prepared on a relatively large scale in good yields from the inexpensive starting materials, EDTA and DTPA.

Attempts to prepare **3** in solvents other than DMSO were unsuccessful. In THF, for instance, the unsymmetrical compound **5** formed, with a hydroxyamide linkage on one end and an amino ester linkage on the other. This compound gave a good analysis for the desired product, but the NMR data combined with the lack of the absorption characteristic of a carboxylic anhydride

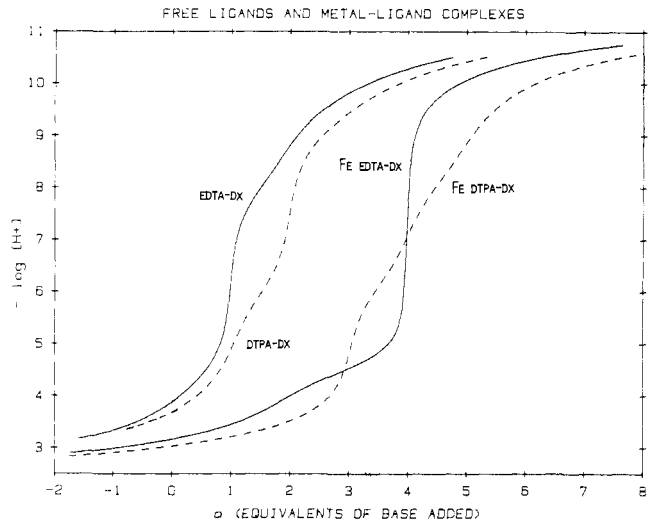

Figure 2. Potentiometric titration curves for *i*-Pr_2EDTA-DX (**3**; 3.3 mM) (continuous lines) and *i*-Pr_2DTPA-DX (**4**; 3.1 mM) (dashed lines). Titrations were run at 25.0 °C at 0.10 M ionic strength (KNO_3) with 0.11 M KOH_3 as titrant. For the titrations of the ferric complexes, 0.95 equiv of Fe^{3+} was present.

in the infrared spectrum indicate it is **5**. It was found that after **5** stood a few days in the NMR solvent (DMSO-d_6) the spectrum changed to that of **3**. Since the dianhydride of EDTA is very insoluble in THF, it may be that the isopropyl substituent prevents the nitrogen from reacting with the dianhydride in the solid state. Since the hydroxylamine may react via the hydroxyl group,[12] and this intermediate is likely to be more soluble, the second hydroxylamine would react to produce **5**. The dianhydride is also largely insoluble in methyl ethyl ketone, methanol, water, and *N*,*N*-dimethylformamide, and products of reactions in these solvents included **5**, EDTA, and EDTA methyl esters.

Ligand Protonation Equilibria. The continuous curves in Figure 2 represent the potentiometric equilibria for **3**, *i*-Pr_2EDTA-DX (H_4L), and **4**, *i*-Pr_2DTPA-DX (H_5L). Both curves show the dissociation of one proton at low pH and of three protons at high pH. The additional proton in DTPA-DX is lost near neutral pH and thus interrupts the break that otherwise separates the two regions. The nonlinear least-squares refinement program BETA (described in detail elsewhere)[14] was used to analyze the data.

(14) Harris, W. R.; Raymond, K. N.; Weitl, F. L. *J. Am. Chem. Soc.* **1981**, *103*, 2667.

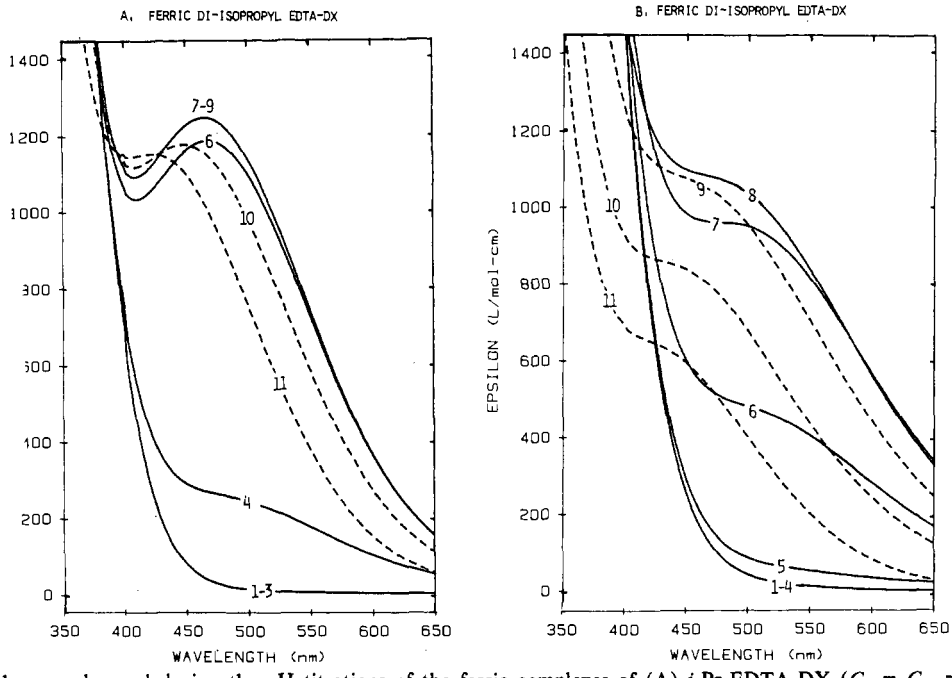

Figure 3. Spectral changes observed during the pH titrations of the ferric complexes of (A) *i*-Pr_2EDTA-DX ($C_L = C_M = 0.07$ mM) and (B) *i*-Pr_2DTPA-DX ($C_L = C_M = 0.09$ mM). Spectra were taken at 25.0 °C at 0.10 M ionic strength (HCl, NaCl) with 10 M NaOH as titrant. They are labeled with pH values.

The resulting protonation constants are represented as log K values in Table I, where

$$K^{H}_{n} = \frac{[H_nL]}{[H][H_{n-1}L]} \quad (1)$$

K_3 and K_4 for EDTA-DX, and K_3, K_4, and K_5 for DTPA-DX. [Note that more than one of the NMR signals are shifted as a result of each protonation (data not shown) so that the assignments of the first three protonations of the ligands are not definite.] The carboxylate protonation constants of the ligands, K_5 and K_6 of *i*-Pr_2EDTA-DX and K_6, K_7, and K_8 of *i*-Pr_2DTPA-DX, were determined by NMR pH titrations in D_2O. The log K values corresponded to the midpoints of the sigmoidal titration curves obtained from a plot of the chemical shifts of the ligand resonances as a function of pH (data not shown). To correct for the substitution of $^2H^+$ for H^+, the following relations were used: log $K^H \approx \log K^D - 0.49$,[15] and pD $\approx$ pH* + 0.4,[16] where pH* is the reading in D_2O obtained from a pH meter calibrated in H_2O. Because the carboxylate protonation constants were not refined, and because approximations were used in the corrections of the constants, we estimate that the error in these values is ±0.5 log unit.

Metal–Ligand Systems. The dashed curves in Figure 2 are potentiometric titration curves for 1:1 mixtures of ferric ion and the ligands. Iron binds over the whole pH range, as is illustrated by the lowering of the curves vs those of the ligands alone. Protonation constants of the metal–ligand systems were determined in the same way as the ligand values and are shown in Table I. It was found that both systems include diprotonated, monoprotonated, and unprotonated species and that an additional proton is lost in basic solution. It was not possible to refine metal–ligand formation constants by potentiometric methods, since even at the lowest pH studied (2.9), the equilibrium concentrations of the complex dissociation species were insensitive to changes in pH (i.e., the amount of free ferric ion present remained negligible).

Spectrophotometric Refinement. It was found that the orange to pink ferric complexes of both ligands absorb strongly in the UV region. While *i*-Pr_2EDTA-DX has a maximum extinction coefficient of 1360 M^{-1} cm^{-1} at 466 nm, the corresponding peak for *i*-Pr_2DTPA-DX appears only as a shoulder to a UV band that tails into the visible region. Figure 3 shows visible spectra for the systems over the pH range studied. The ultraviolet absorption is not as strongly affected by the protonation behavior.

A nonlinear least-squares refinement program, REFSPEC, was used to determine equilibrium constants from the spectrophotometric data. This program is described in detail elsewhere,[17] so that only the essentials are mentioned here. The spectrophotometer measures absorbances for 251 wavelengths for 350 to 800 nm. Each spectrum (A_i) is stored as a 251-dimensional vector. If the total number of spectra recorded during the titration is m, then A is the resultant 251 by m matrix. If there are n species in solution that contribute to the absorbance spectra and if Beer's law is obeyed, then there are only n linearly independent spectra and the other $m - n$ spectra are linear combinations of these. The first task of the refinement procedure is to characterize the number of species n, subject to the error limits composed by the experimental data. This corresponds to determining the rank of the absorbance matrix (see the Appendix).[18-20] Next, the spectra of the solution species are determined and calculated values for the absorbance values are obtained. The equilibrium constants for these species are refined by a least-squares procedure, which minimizes the sum of the squared residuals between the observed and calculated spectra.

To be assured of the accuracy and consistency of the spectrophotometric refinement for the ferric systems, two titrations using different conditions were performed for the metal complexes of both ligands. To refine the protonation equilibria of **3**, the wavelength range from 350 to 800 nm was used, whereas the refinement range for **4** was 400 to 800 nm. Five components were used in each case resulting from the five absorbing species expected to be present: Fe^{3+}, MH_2L, MHL, ML, and MLOH. The values obtained from the two sets of refinements were averaged and are in good agreement with the potentiometric results (Table I). Figures 4 and 5 show the extinction coefficient spectra and species

(15) Schowen, R. L.; Schowen, K. B. L. *Methods Enzymol.* **1982**, *87*, 551.
(16) Glasoe, P. K.; Long, F. A. *J. Phys. Chem.* **1960**, *64*, 188.
(17) Scarrow, R. C. Ph.D. Dissertation, University of California, Berkeley, CA, 1985.
(18) See, for example: Hartley, F. R.; Burgess, C.; Alcock, R. *Solution Equilibria*; Halsted: New York, 1980; *Factor Analysis in Chemistry*; Wiley-Interscience: New York, 1980.
(19) Maeder, M.; Gampp, H. *Anal. Chim. Acta* **1980**, *122*, 303.
(20) Mardia, K. V.; Kent, J. T.; Bibby, J. M. *Multivariate Analysis*; Academic: London, 1979; Chapter 8.

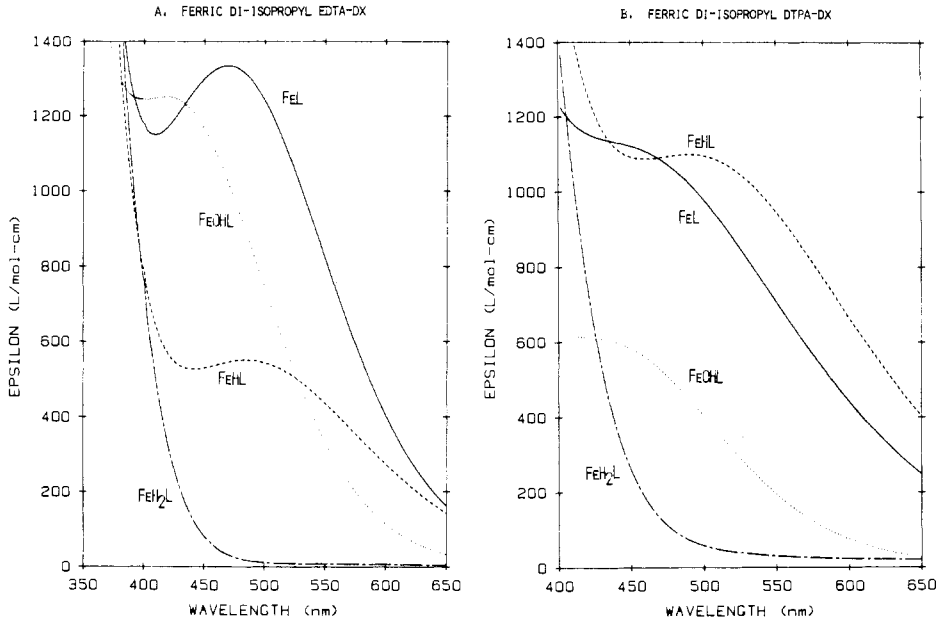

Figure 4. Extinction coefficient spectra of the ferric species of (A) *i*-Pr_2EDTA-DX and (B) *i*-Pr_2DTPA-DX calculated from the results of the spectrophotometric refinements.

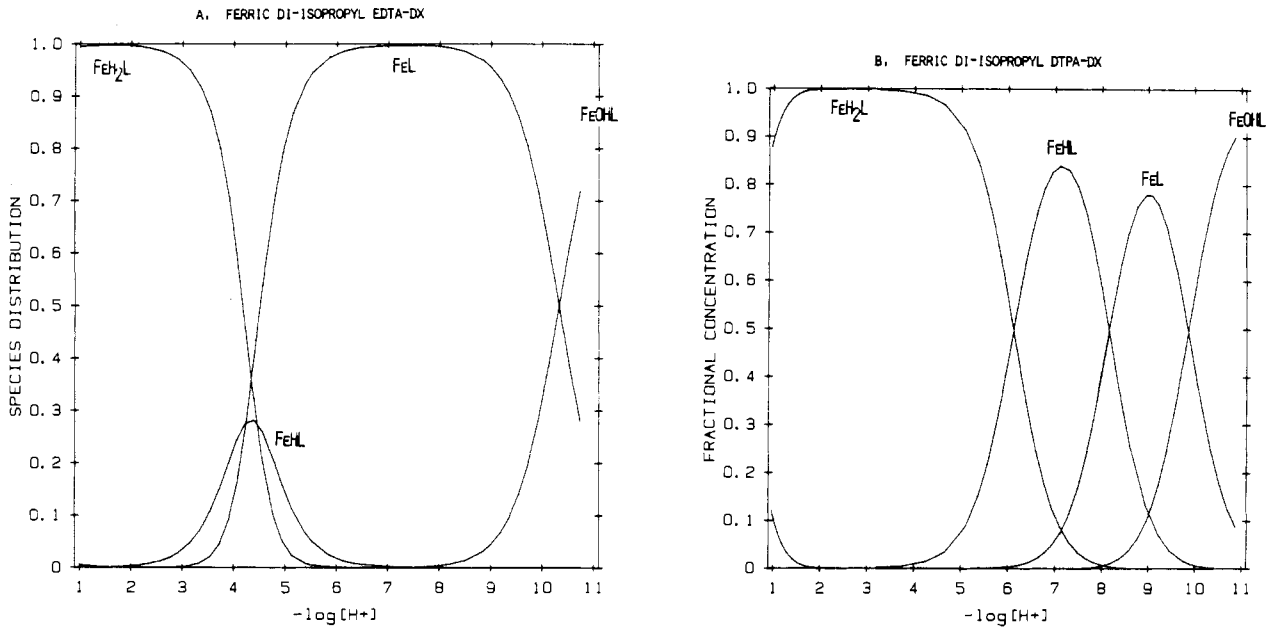

Figure 5. Species distribution curves for (A) *i*-Pr_2EDTA-DX and (B) *i*-Pr_2DTPA-DX.

distributions calculated for the metal–ligand systems from the refinements.

Although the set of titrations in the visible region included data at very low pH (1.0), the amount of free iron present in both systems was still too low to allow direct refinement of the metal–ligand formation constants, since an excess of ligand was used. When ligand was added to a ferric solution at pH 1, and the absorbance plotted vs the amount of ligand added, it was seen that the absorbance rose in a linear fashion until 1 equiv of ligand was added, whereupon the slope flattened out. The break at 1 equiv was not sharp, however, but slighly curved. These data (23–24 spectra) were analyzed by using three components (absorbing species are Fe^{3+}, MH_2L, and the fully protonated ligand) from 231 to 500 nm, which is where the largest spectral changes occurred. The metal–ligand formation constants can be determined from the cumulative equilibrium constant

$$\beta_{MH_2L} = \frac{[MH_2L]}{[M][L][H]^2} \qquad (2)$$

obtained from these refinements. The results are listed in Table I. Also shown are the spectral changes observed as **4** is added to ferric ion (Figure 6) and a plot of the observed and calculated extinction coefficients of the major component of the titration of ferric ion with **4** vs the amount of ligand added (Figure 7) to show the curvature and to exemplify the fit of the refinements. There is less free metal present for the system of **3** at pH 1, so that there is less curvature, and a higher estimated standard deviation.

The last deprotonations of the ferric complexes have been assigned to the formation of FeOHL complexes. A plot of the hydrolysis constant, log K_{OH}, vs the formation constant, log K_{ML}, for the ferric complexes of a number of ligands related to *i*-Pr_2EDTA-DX and *i*-Pr_2DTPA-DX has been shown empirically to yield a straight line.[21] The data for both **3** and **4** fit well on this line, supporting the species assignment.

Discussion

Ligand Protonation Constants. The value of log K_1, 10.56 for *i*-Pr_2EDTA-DX and 10.85 for *i*-Pr_2DTPA-DX, are unusually high

(21) Harris, W. R.; Carrano, C. J.; Raymond, K. N. *J. Am. Chem. Soc.* **1979**, *101*, 2722.

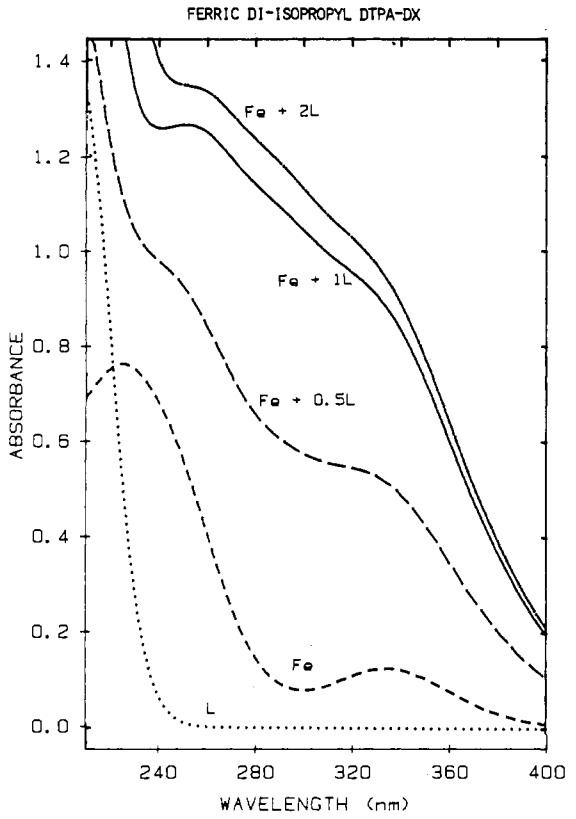

Figure 6. Spectral changes observed during the titration of Fe^{3+} (0.15 mM) with *i*-Pr_2DTPA-DX (5.0 mM) at 25 °C at pH 1 and constant ionic strength (0.10 M HCl).

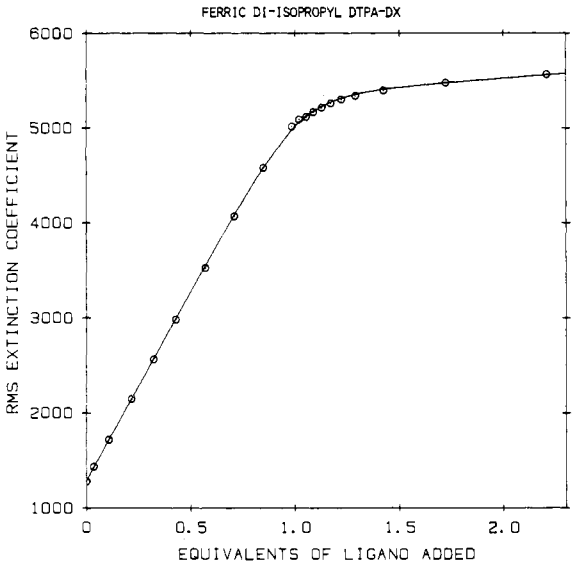

Figure 7. Calculated (continuous line) and observed (circles) absorbances of the major component of the titration described in Figure 6. The *y* axis represents absorbance values normalized by C_{Fe}. Note the curvature upon the addition of 1 equiv of DTPA-DX.

for hydroxamic acids, which usually exhibit log *K* values of 8.1 to 10.0.[22] Hydrogen bonding of the hydroxamate proton to the nearest amine nitrogen apparently makes the first protonation of the ligands more favorable than usual. The amine and carboxylate protonations are typical of the amine carboxylates,[23] occurring in the ranges of pH 3.5 to 9.5, and pH −0.5 to 2.5, respectively.

The behavior of the chemical shifts of the ligand resonances as a function of pH is very similar to that of the parent compounds, EDTA and DTPA, which has been discussed by Letkemann and Martell.[24]

Metal Protonation Constants. The protonations determined by potentiometric and spectrophotometric methods differ only slightly. The maximum discrepancy is 0.13, and the average is 0.06. Not only is this good agreement between the techniques but it also indicates that the equilibria studied are independent of total iron and ligand concentrations, which are 35 times greater in the potentiometric titrations. This confirms that the complexes studied are 1:1 in iron and ligand. The protonation constants of the ferric DTPA-DX complex are higher than those of the EDTA analogue. The FeL complex of *i*-Pr_2DTPA-DX is a dianion, which is more easily protonated than the monoanionic ferric EDTA-DX complex. It is interesting that the second protonation constant of the iron(III) complex of *i*-Pr_2EDTA-DX is higher than the first. This result was consistently obtained by both the potentiometric and spectrophotometric methods with a correlation coefficient between the two constants of 0.34 or less. This implies a major change in the structure of the complex, which makes the second protonation of the ligand more favorable.

Visible Spectra. Hydroxamate complexes of iron(III), which are coordinated as shown in **6**, have characteristic ligand-to-metal charge-transfer absorptions in the visible region. Monohydroxamate complexes absorb at 500–530 nm with an extinction coefficient of 900–1100 M^{-1} cm^{-1}, and dihydroxamate complexes show bands at 470–480 nm (1750–2100 M^{-1} cm^{-1}).[21] In contrast, ferric complexes of polycarboxylate ligands absorb at higher energy and appear only slightly yellow. The λ_{max} value of the *i*-Pr_2EDTA-DX·FeL complex, 466 nm, characterizes it as a dihydroxamate complex, although the extinction coefficient, 1360 M^{-1} cm^{-1}, is lower than expected. On the other hand, the FeH_2L complex of the ligand has no feature in the visible region. This suggests that the coordination around the iron changes from a dihydroxamate coordination to an EDTA-like coordination as two protons are added. The FeHL species, which is never more than a minor component (see Figure 5), is likely to be a monohydroxamate complex.

The ferric *i*-Pr_2DTPA-DX system differs significantly. The ligand has a large number of coordination sites available, two hydroxamates, three carboxylates, and three tertiary amines; a dihydroxamate complex does not appear to form at all. The spectrum of the FeHL species (500 nm, 1100 M^{-1} cm^{-1}) characterizes it as a monohydroxamate complex, but the shoulder in the visible spectrum of the FeL species (~460 nm, 1100 M^{-1} cm^{-1}) cannot be easily assigned. It is possible that the complex begins to hydrolyze before the ligand is completely deprotonated, such that the FeL species is actually Fe(OH)(HL). As in the EDTA-DX case, the FeH_2L species does not include any hydroxamate coordination.

Molecular models indicate that **3** can coordinate an octahedral iron atom by formation of five-membered chelate rings involving either both hydroxamate or both glycyl functional groups, which presumably represent structures of FeL and FeH_2L. However, it is impossible to construct a space-filling model of FeHL with **3** bound via a hydroxamate and via a glycyl group from either the same or the opposite side of the ligand. Thus protonation and decomplexation of *both* hydroxamates are prompted by the formation of the three five-membered chelate rings of EDTA-like coordination, while protonation and decomplexation of a *single* hydroxamate does not result in any new coordination of small chelate rings. The tendency of FeHL to disproportionate can therefore be explained by the reduced number of small chelate rings in this molecule compared with that in either FeL or FeH_2L. (It is possible, on the basis of molecular modeling, that one or both carboxylates bind in FeHL, but this results in larger, less favored chelate rings.)

Formation Constants. The FeL complex of *i*-Pr_2DTPA-DX is slightly less stable than that of *i*-Pr_2EDTA-DX. The FeL complex

(22) Anderegg, G.; L'Eplattenier, F. L.; Schwarzenbach, G. *Helv. Chim. Acta* **1963**, *156*, 1400.

(23) Martell, A. E.; Smith, R. M. *Critical Stability Constants*; Plenum: New York, 1974, 1981; Vols. 1, 5.

(24) Letkemann, P.; Martell, A. E. *Inorg. Chem.* **1979**, *18*, 1284.

Table II. Comparative Formation Constants and pM Values of Selected Ferric Complexes

ligand	log K_{ML}	pM_1[a]	pM_2[b]	pM_3[c]
enterobactin[d]	52	37.6	35.5	23–26
trihydroxamates[d]	29–32	27–30	25–28	23–26
transferrin[d]		25.6	23.6	21.4
i-Pr_2EDTA-DX[e]	30.2	27.0	25.0	22.9
i-Pr_2DTPA-DX[e]	29.7	25.6	23.6	22.9
aerobactin[d]	22.93	25.4	23.3	21.2
rhodotorulic acid[d]	21.99	25.0	21.9	20.9

[a] Conditions: C_{Fe} = 1 μM, C_L = 1 mM, pH 7.40. [b] Conditions: C_{Fe} = 1 μM, C_L = 10 μM, pH 7.40. [c] Conditions: C_{Fe} = 1 μM, C_L = 1 mM, pH 6.00. [d] See ref 5. [e] This work.

of the DTPA-derived ligand is a dianion whereas the *i*-Pr_2EDTA-DX complex is monoanionic. Furthermore, the DTPA-DX ligand is more bulky. Both factors may weaken this ligand's complexing ability. The ferric complex formation constant of *i*-Pr_2EDTA-DX is 5 orders of magnitude higher than that of EDTA (log K_{ML} = 25.0),[24] whereas the K_{ML} value of *i*-Pr_2DTPA-DX is only 2 orders of magnitude higher than that of DTPA (log K_{ML} = 27.8).[24] It is noteworthy that the formation constant of the iron(III) complex of *i*-Pr_2EDTA-DX is 8 orders of magnitude higher than that reported for the unsubstituted EDTA-DX, ethylenedinitrilo-*N*,*N*′-diacethydroxamic-*N*,*N*′-diacetic acid (**2**; log K_{ML} = 22.15).[9] A possible explanation for this difference is that the hydrogen on the hydroxamic acid group of unsubstituted EDTA-DX forms a stable hydrogen bond with the neighboring tertiary amine in a five-membered ring. This hydrogen bond needs to be broken to enable the formation of a ferric complex, thus destabilizing the latter.

Recently, the ferric complex formation constants of two dihydroxamate macrocycles have been determined.[25] The better of the two ligands, **7**, which contains the same functional groups as *i*-Pr_2EDTA-DX, has a formation constant (log K_{ML} = 24.45) that is 5 orders of magnitude lower than that of *i*-Pr_2EDTA-DX. Although **7** is an endocyclic dihydroxamate, it seems to be too bulky to be highly effective as a ferric ligand. Table II lists the formation constants of the 1:1 ferric complexes of selected ligands in comparison with those of *i*-Pr_2EDTA-DX and *i*-Pr_2DTPA-DX. Values for *i*-Pr_2EDTA-DX and *i*-Pr_2DTPA-DX are higher than those for the dihydroxamate siderophores aerobactin and rhodotorulic acid. They are closer to the values observed for trihydroxamate siderophores.

As we have noted,[2] a more meaningful comparison of the effectiveness of a ligand is the equilibrium free metal concentration, expressed as −log [Fe^{3+}] (pM). This value takes into account dilution effects as well as proton competition for the ligand. The pM values for *i*-Pr_2EDTA-DX and *i*-Pr_2DTPA-DX and other ligands at various near-physiological conditions are listed in Table II. *i*-Pr_2EDTA-DX is seen to be more effective than the dihydroxmate siderophores. It is also thermodynamically capable of removing iron from the human serum protein transferrin, especially when used at higher concentrations. *i*-Pr_2DTPA-DX is more effective than either aerobactin or transferrin only below physiological pH, since the protonated ligand forms are very stable.

Iron and Plutonium Removal. Ligands such as *i*-Pr_2EDTA-DX and *i*-Pr_2DTPA-DX are promising candidates for chelation therapy for iron and plutonium. The dihydroxamate siderophore rhodotorulic acid has been shown to be effective as an iron removal agent in human patients and is somewhat orally active; however, treatment with rhodotorulic acid involves painful side effects.[7] The octadentate ligand DTPA is also known to be an effective plutonium removal agent in human beings, although it too has side effects.[8] Its toxicity is much reduced when it is coadministered with calcium or, especially, zinc.[8] One of the ligands described here, *i*-Pr_2DTPA-DX (**4**), has recently been studied in an in vivo mouse screen and was found to be an effective iron removal agent in mice.[26] Unfortunately, the treatment exhibited side effects similar to those observed for DTPA.

i-Pr_2EDTA-DX (**3**), which is a more effective iron chelate than the DTPA analogue in vitro, may be more effective for in vivo iron removal as well. Since it has fewer carboxylates and amines available for binding divalent metals, it should prove to be more selective for iron removal, and therefore less toxic, than *i*-Pr_2DTPA-DX. Plutonium removal studies in mice have shown that the calcium salt of *i*-Pr_2DTPA-DX is slightly more effective than Ca-DTPA.[27] *i*-Pr_2EDTA-DX, which is optimally hexadentate, is significantly less effective than Ca-DTPA.[27]

This study shows that nitriloacetic acids such as EDTA or DTPA can easily be derivatized by using alkylhydroxamic acids to form dihydroxamate chelating agents that compare well with corresponding siderophores and exhibit good solubility properties. They do not show the specificity for Fe(III) of some of the catecholate ligands, but their ready synthesis makes them promising for practical applications.

Acknowledgment. We thank Dr. P. Durbin, N. Jeung, and Dr. H. Metivier for discussing their in vivo Pu removal experiments. This research was supported by the National Institutes of Health under Grant No. AM 32999.

Appendix

The program REFSPEC is written in FORTRAN for an IBM-PC microcomputer. The program itself is described elsewhere, along with a listing of the source code.[16] The mathematical basis of the analysis has been derived elsewhere,[18] and other applications of this approach have been implemented.[17] The algorithm employed by REFSPEC involves principal component analysis[19] to determine the minimum number of absorbing species that must be assumed to model the absorbance data. As a result of this analysis, the absorbance data are condensed to a smaller number of dependent variables, which can be used in the subsequent least-squares refinement of the equilibrium constants and absorption spectra of the individual species in solution.

Let n_λ be the number of individual wavelength values used in the digital storage of the absorption spectra. If m is the number of spectra recorded, then the absorbance data can be described by the (n_λ by m) matrix $\mathbf{A}^o$, in which the column vectors $\mathbf{A}_i$ correspond to the absorbance values for the ith spectrum. If Beer's law holds, the calculated spectra are sums of the spectra of the n absorbing species in solution, weighted by their concentrations. The extinction coefficient matrix $\mathbf{E}$ is then an (n_λ by n) matrix whose column vectors are in the extinction coefficient spectra of the individual components in solution. The (n by m) matrix of concentrations, $\mathbf{C}$, is composed of column vectors that correspond to the concentrations of the n absorbing species under the experimental conditions when a given spectrum is recorded. The (n_λ by m) matrix of the calculated spectra, $\mathbf{A}^c$, is then determined by Beer's law:

$$\mathbf{A}^c = \mathbf{EC} \tag{A1}$$

The observed and calculated spectra will differ, even when the extinction coefficient and concentration data are shown, by experimental errors R_{ij}, for the ith wavelength value and the jth spectrum, or in matrix form:

$$\mathbf{A}^o = \mathbf{A}^c + R \tag{A2}$$

In principle, the least-squares refinement of the values for the extinction coefficients (the elements of $\mathbf{E}$) and the equilibrium constants (which determine the elements of the concentration matrix $\mathbf{C}$) could proceed by standard minimization of the residual:

(25) Sun, Y.; Martell, A. E.; Motekaitis, R. J. *Inorg. Chem.* **1985**, *24*, 4343.

(26) Rosenkrantz, H.; Metterville, M. A. "In Vivo Mouse Bioassay of Potential Iron Chelators"; Report No. MRI-CA 03-85-01B; EG&G Mason Research Institute: 57 Union St., Worchester, MA 01609, 1985; Bioassay 42, Compound No. X294 (submitted to National Institutes of Arthritis, Diabetes and Digestive and Kidney Diseases, Hematology Program under Grant No. NO1-AM-0-2206).

(27) Durbin, P. W.; Jeung, N.; Raymond, K. N.; White, D. L.; Rodgers, S. J.; Turowski, P. N. *Division of Biology and Medicine Annual Report*; Lawrence Berkeley Laboratory: Berkeley, CA, 1986; LBL-20345.

$$r^2 = \sum_{i=1}^{n_\lambda} \sum_{j=1}^{m} R_{ij}^2 / mn_\lambda \quad \text{(A3)}$$

The resultant r should be equal to or greater than the standard deviation of a single absorption measurement, σ_0 (typically about 0.0003 absorbance unit). While this refinement could proceed directly by using eq A1–A3, this leaves the (n_λ by n) **E** matrix and the equilibrium constants as the parameters and the (n_λ by m) $\mathbf{A}^c$ matrix as the observations. For refinement we need each derivative of the type d(observation)/d(variable parameters). Even if the derivatives involving equilibrium constants are ignored, there are $n_\lambda^2 mn$ such derivatives.

This is an impractically larger amount of computation for a small computer. This approach would also lead to some numerical problems because of the high correlation between the extinction coefficient values. Using principal component analysis,[18,16] it is possible to condense the absorbance data to a smaller number of "observations" in the refinement procedure. Consider, for example, a system where there are three species in solution that contribute to the absorption in the wavelength range studied. If four of the spectra were recorded at four equally spaced wavelengths, the absorbance data could be represented as a 4 by 4 matrix. However, the determinant of this matrix, to within error limits of the experiment, will be zero, since only three of the absorbance spectra are linearly independent. That is, the rank of this matrix would be 3 (the rank being the number of linearly independent rows or columns of the matrix).[18] A more typical example, with data from the HP8450A spectrometer, would be about 50 spectra, each composed of about 200 absorbance values at discrete wavelengths. However, if there are only three absorbing species, the rank of this matrix remains 3.

The n columns of **E** span an n-dimensional subspace. Since the columns of $\mathbf{A}^c$ (the calculated spectra) are vectors that are linear combinations of the columns of **E** (the extinction coefficient spectra), the subspace can also contain all columns of $\mathbf{A}^c$. This subspace can be characterized by n orthonormal vectors $\mathbf{V}_i$ such that the (n_λ by n) matrix **V** satisfies the relation

$$\mathbf{E} = \mathbf{VZ} \quad \text{(A4)}$$

$$\mathbf{A}^c = \mathbf{VY}^c \quad \text{(A5)}$$

Here **Z** (n by n) and **Y** (n by m) are scaling matrices that take the "normalized component spectra" of **V** to extinction coefficients and absorbance values in the same way that the i values scale the species concentrations to absorbance. Since **V** is orthonormal, its product with its transpose ($\mathbf{V}^T$) gives an (n by n) identity matrix **I**

$$\mathbf{V}^T\mathbf{V} = \mathbf{I} \quad \text{(A6)}$$

and hence

$$\mathbf{Y}^c = \mathbf{V}^T\mathbf{A}^c \quad \text{(A7)}$$

This matrix $\mathbf{Y}^c$ can now be regarded as a condensed version of the calculated absorbance spectra. Initially, $\mathbf{Y}^c$ and $\mathbf{A}^c$ (and **E** and **C**) are unknown. However, by analogy to eq A7 one may define matrix $\mathbf{Y}^o$ on the basis of the data $\mathbf{A}^o$:

$$\mathbf{Y}^o = \mathbf{V}^t\mathbf{A}^o \quad \text{(A8)}$$

Here $\mathbf{Y}^o$ represents a condensed form of the observed absorbance data. We can define the componentization error matrix, $\mathbf{R}^*$, such that

$$\mathbf{A}^o = \mathbf{VY}^o + \mathbf{R}^* = (\mathbf{VV}^T)\mathbf{A}^o + \mathbf{R}^* \quad \text{(A9)}$$

The matrix $\mathbf{VY}^o$ is $\mathbf{A}^o$ after projection into the n-dimensional space defined by **V** (note that $\mathbf{VV}^T$ is a projection operator). The normalized component spectra, **V**, can be estimated[19] by minimizing r^*, where r^* is determined by eq A3, with R_{ij} replaced by R^*_{ij} and r replaced by r^*.

The componentization process is begun by assuming that there is only one absorbing species, i.e., that $n = 1$. If $r^* \gg \sigma_0$, and particularly if systematic wavelength-dependent trends are noted in the error spectra $\mathbf{R}^*_i$ (column vectors of $\mathbf{R}^*$), then one concludes that there are more species present and the process is repeated with n incremented by 1. When eq A8 is able to reduce r^* to about σ_0 and the column vectors of $\mathbf{R}^*$ are essentially featureless, then the process is stopped and this n is chosen as the number of species in solution.

The orthonormal coefficient spectra of **V** are further used by REFSPEC to determine the equilibrium constants of the solution species and their spectra. The equilibrium constants interrelating the solution concentrations are refined by using the following equation, derived from eq A1 and A5:

$$\mathbf{Y}^c = \mathbf{ZC} \quad \text{(A10)}$$

Starting values of the concentrations, calculated from the trial equilibrium constants and the analytical concentrations of the total metal, total ligand, and acid, give trial values for **C**. This and the trial values for **Z** allow for trial calculations of $\mathbf{Y}^c$ using eq A10. The actual refinement procedure then minimizes the sum of the squared differences between the "observed" matrix $\mathbf{Y}^o$ and the "calculated" values $\mathbf{Y}^c$.

In the earlier example of direct least-squares refinement of all absorbance values, over 10^7 derivatives would have to be calculated for $n_\lambda = 200$, $m = 50$, and $n = 5$. In contrast, refinement using eq A8 and A10 has the (n by n) **Z** matrix as the parameters and the (n by m) matrix $\mathbf{V}^T\mathbf{A}$ as the observations. This gives mn^3 as the number of derivatives, or 6250 for the example shown. Not only does this result in a great savings of computer time but it also gives a much better conditioned least-squares problem. After each cycle of refinement, new values for **Z** and new values for **C** (from the new equilibrium constants) are calculated and the process is iterated to convergence. After the refinement, the extinction coefficients are calculated by using eq A4.

Registry No. **3**, 111557-57-4; **4**, 111557-58-5; **5**, 111557-59-6; EDTA dianhydride, 23911-25-3; DTPA dianhydride, 23911-26-4; *N*-isopropylhydroxylamine, 5080-22-8.